ISSN 1066-3622, Radiochemistry, 2022, Vol. 64, No. 2, pp. 211–218. © Pleiades Publishing, Inc., 2022.

Radiocomplexation and Biological Evaluation of [^{99m}Tc]Tricarbonyl Rabeprazole as a Radiotracer for Peptic Ulcer Localization

M. H. Sanad[a,b,*], F. A. Marzook[a], S. K. Mandal[c], and M. Baidya[d,e]

[a] *Labeled Compounds Department, Hot Laboratories Center, Egyptian Atomic Energy Authority, Cairo, PB 13759 Egypt*
[b] *Department of Physics and Engineering Mathematics, Faculty of Engineering, Ain Shams University, Cairo, 11566 Egypt*
[c] *Department of Pharmaceutical Chemistry, Dr. B.C. Roy College of Pharmacy and Allied Health Sciences, Durgapur, West Bengal, 713206 India*
[d] *Bharat Pharmaceutical Technology, Amtali, Agartala, Tripura, 799130 India*
[e] *JIS University, Kolkata, West Bengal, 700109 India*
**e-mail: drsanad74@gmail.com*
Received June 4, 2021; revised October 28, 2021; accepted November 2, 2021

Abstract—The radiotracer [^{99m}Tc]tricarbonyl Rabeprazole was successfully prepared using the [^{99m}Tc]tricarbonyl precursor. The reaction conditions were optimized (200 μg/2 mL substrate concentration, pH 8, incubation temperature 100°C, 30 min) to achieve the maximum radiochemical purity of 98%. Thin layer chromatography (TLC) and high-performance liquid chromatography (HPLC) were used to assess the radiochemical purity and quality control parameters. A biodistribution study was also conducted to evaluate the biological biodistribution of [^{99m}Tc]tricarbonyl Rabeprazole in three different groups of mice models, with the normal group serving as the control and the second and third groups being microbial and chemically induced stomach ulcer disease models, respectively. The radiotracer [^{99m}Tc]tricarbonyl Rabeprazole complex was administered intravenously into mice via the tail vein and dissected at predefined time intervals. The biodistribution data demonstrated that the maximum absorption of [^{99m}Tc]tricarbonyl Rabeprazole complex in the stomach of normal mice and microbially and chemically induced ulcerated mice were 9.5, 35.3, and 23.7% ID/g tissue at 1 h post injection, respectively. The outcomes of the research show that [^{99m}Tc]tricarbonyl Rabeprazole can be used as a promising imaging agent to diagnose stomach ulcers.

Keywords: Rabeprazole, [^{99m}Tc]tricarbonyl precursor, labeling, *Helicobacter pylori*

DOI: 10.1134/S1066362222020138

INTRODUCTION

Rabeprazole, 2-[4-(3-methoxypropoxy)-3-methyl-2-pyridinyl]methylsulfinyl-1H-benzimidazole, is a proton pump inhibitor that inhibits the H^+/K^+ ATPase and thus suppresses both basal and induced stomach acid secretion. However, proton pump inhibitors are inadequate for controlling gastric acidity, particularly in gastroesophageal reflux disease (GERD). Therefore, a combination therapy with H_2 receptor blockers and proton pump inhibitors is employed to regulate intragastric pH better than proton pump inhibitors alone [1]. Rabeprazole is also used to treat peptic ulcers, duodenal ulcers, and dyspepsia [2, 3]. There have been several studies on stomach ulcer imaging [4–15], but none of them compare radiotracer biodistribution in chemical and microbiological stomach ulcer models. In this study, we use a Helicobacter pylori induced stomach ulcer model (microbiological model) to address the shortcomings in this critical area [16–33]. Technetium-99m is regarded as the most often used radionuclide due to its acceptable half-life ($T_{1/2}$ = 6.01 h), γ-ray energy (140 keV, 89.4%) ideal for SPECT, and relatively low abundance of β-emission [16]. The objective of this paper is to optimize the preparation of the radiotracer, [^{99m}Tc]tricarbonyl Rabeprazole, to overcome the drawbacks of the previous radiotracers [4–15]. In a biodistribution investigation, normal, microbially, and chemically ulcerated Swiss Albino mice were used to assess the radiotracer uptake in the stomach of each model at the same time.

EXPERIMENTAL

General. Rabeprazole was a gift from Pharaonia Company for Pharmaceutics. Pertechnetate [$^{99m}TcO_4^-$] was eluted from Elutec Brussels (Belgium) $^{99}Mo/^{99m}Tc$ generator; all the other chemicals and solvents were purchased from Merck (Kenilworth, NJ, the United States). The National Research Centre provided H. pylori as a gift (Cairo, Egypt). Thin layer chromatography (TLC) aluminum sheets (20 × 25 cm) SG-60 F254 were supplied by Merck. Unless otherwise specified, all compounds were of analytical or clinical grade and were used immediately without further purification. A well-type NaI scintillation γ-counter, model Scaler Ratemeter SR7 (Nuclear Enterprises Ltd., the United States), was used for radioactive measurement. The Shimadzu reversed-phase HPLC (RP-HPLC) system includes LC-9A pumps, a Rheodyne injector, a UV spectrophotometer detector (SPD-6A), and a reversed-phase column (RP-18, 250 × 4.6 mm, 5 μm, Lichrosorb). The chromatograms were obtained by fraction collection, and the corresponding data were obtained by fitting the discrete data using the Origin software.

Radiosynthesis of ^{99m}Tc-tricarbonyl precursor. The [^{99m}Tc]tricarbonyl precursor, fac-[$^{99m}Tc(CO)_3(H_2O)_3$]$^+$, was synthesized using the method described earlier [16–21]. The radiosynthesis yield and stability of the [^{99m}Tc]tricarbonyl precursor were determined using 0.22 μm Millipore filtration followed by RP-HPLC analysis.

Radiolabeling to obtain [^{99m}Tc]tricarbonyl Rabeprazole. The reaction mixture volume was set at 2000 μL. At room temperature, 200 μg Rabeprazole dissolved in ethanol (1 mg : 1 mL) was added to 1 mL of the synthesized [^{99m}Tc]tricarbonyl precursor, after which 100 μL of potassium phosphate buffer solution (pH 8) was added. Then, the reaction mixture was heated at 100°C for 30 min. After cooling to 37°C (using a thermostatically controlled water bath), radio-HPLC was used to determine and verify the radiolabeling yield [21].

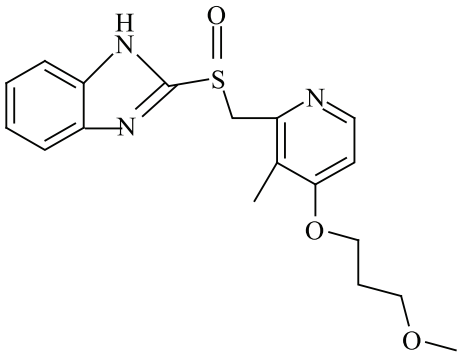

Rabeprazole

Radio-HPLC of [^{99m}Tc]Tricarbonyl Rabeprazole. A 10 μL aliquot of the reaction mixture containing [^{99m}Tc]tricarbonyl Rabeprazole was injected into the RP-18 column. The analysis of the [^{99m}Tc]tricarbonyl Rabeprazole mixture was performed using the gradient elution with 0.05 M triethylammonium phosphate (TEAP) (pH 2.8, solvent A) and methanol (solvent B) at the detection wavelength of 280 nm and flow rate of 0.6 mL/min. The gradient elution was used according to previous studies: isocratic elution (100% A), 0–5 min; linear gradient from 100% A/0% B to 75% A/25% B, 5–8 min; linear gradient from 75% A/25% B to 66% A/34% B, 8–11 min; linear gradient from 66% A/34% B to 0% A/100% B, 11–22 min; and isocratic elution (100% B), 22–25 min [17–20].

TLC analysis. TLC analysis was used to determine the radiochemical yield of the radiotracer, [^{99m}Tc] tricarbonyl Rabeprazole. In brief, the TLC-SG sheets were marked with a non-pointed pencil at 2 cm above the base lines into 1 cm fragments up to 14 cm. The reaction mixture was then filtered through a Millipore filter (0.22 μm), and 5 μL of it was applied using a micropipette. In a closed jar containing acetonitrile as the developing solvent, the sheets were developed in an ascending fashion. After the development, the TLC-SG sheets were removed, dried, and cut into 1 cm wide strips, which were then counted with a γ-counter. The reaction mixture was filtered through a 0.22 μm Millipore filter before TLC analysis to remove any possible colloid. The radiochemical conversion to [^{99m}Tc]tricarbonyl Rabeprazole was determined using aluminum-backed silica gel GF 254 plates [34, 35].

Stability in rat serum media. TLC and HPLC procedures were used to study the stability of the radiotracer, [^{99m}Tc]tricarbonyl Rabeprazole, in rat serum. Briefly, 0.2 mL of [^{99m}Tc]tricarbonyl Rabeprazole solution [0.15×10^{-3} GBq] was mixed with 1.8 mL of normal rat serum by volume and kept at 37°C. To test the stability of [^{99m}Tc]tricarbonyl Rabeprazole, the mixture was examined using TLC and HPLC at various time intervals [56–70]. The radioactivity was counted using a well-type γ-scintillation counter.

Biodistribution and animal studies. The biodistribution of [^{99m}Tc]tricarbonyl Rabeprazole was

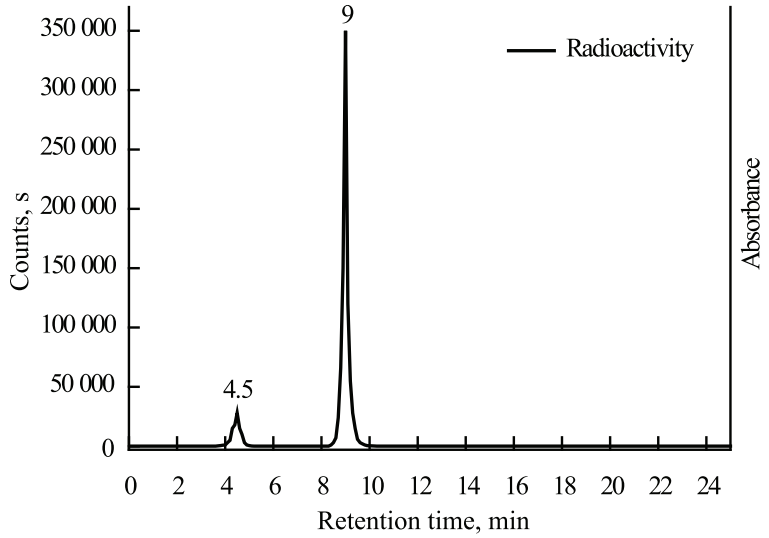

Fig. 1. HPLC radiochromatograms: (a) [^{99m}Tc]tricarbonyl precursor (R_t = 4.7 min; the peak at R_t = 11.6 min belongs to free [^{99m}Tc]pertechnetate) and (b) reaction mixture containing [^{99m}Tc]tricarbonyl Rabeprazole (R_t = 6 min; the peak at R_t = 4.5 min belongs to free [^{99m}Tc]tricarbonyl.

investigated in Swiss Albino mice weighing about 40–50 g. The Ethical Committee of the Labeled Compounds Department approved the experimental protocol. An H. pylori-induced microbiological model of stomach ulcer was developed using the method described by Duangporn [26]. Briefly, mice were pretreated for three days with streptomycin suspended in tap water (5 mg/mL). After that, the mice were gavaged with H. pylori bacterial suspension (5×10^{-8} CFU/mL) twice daily at a 4-h interval for three days. Two weeks following injection, the biodistribution of [^{99m}Tc]tricarbonyl Rabeprazole, including stomach ulcer uptake, was evaluated in this group. In addition, the biodistribution of the radiotracer in the chemically induced ulcer-bearing mice model was studied following the procedure described earlier [4, 5]. Mice were divided into three groups (control and microbiologically and chemically induced ulcer-bearing groups) to give 60 mice in total (five mice per experimental point, n = 5). Each animal in the groups was intravenously injected with 0.2 mL (200–300 kBq) of [^{99m}Tc]tricarbonyl Rabeprazole solution adjusted to physiological pH via the tail vein and sacrificed at various times after injection (5 min, 30 min, 60 min, and 2 h). All organs were separated and examined to determine the amounts of [^{99m}Tc]tricarbonyl Rabeprazole in comparison to the reference solution of the labeled substrate. Fresh blood, bone, and muscle samples were also collected and evaluated. The average percentage of the administered dose per gram was calculated. The blood, bone, and muscle weights were assumed to be 7, 10, and 40% of total body weight, respectively [71–90]. Corrections for the background radiation and decay were done during the experiments. The one-way ANOVA test was used to evaluate the data. The mean standard deviation was used to present all of the results. P values less than 0.05 were considered statistically significant.

RESULTS AND DISCUSSION

TLC analysis. The radiotracer, [^{99m}Tc]tricarbonyl Rabeprazole, had an R_f value of 0.9–1.0, while the R_f values for [$^{99m}TcO_4^-$] and [^{99m}Tc]tricarbonyl core were 0.3–0.4. The radiochemical yield of the [^{99m}Tc]tricarbonyl Rabeprazole complex, calculated by subtracting the relative percent content of [$^{99m}TcO_4^-$] and [^{99m}Tc]tricarbonyl core from 100%, immediately after the synthesis was over 98% [91–95].

Evaluation of radiochemical yield by HPLC. The HPLC chromatogram (Fig. 1a) showed sharp peaks of free [^{99m}Tc]pertechnetate and [^{99m}Tc]tricarbonyl with R_t 4.7 and 11.60 min, respectively. The [^{99m}Tc]tricarbonyl precursor was successfully synthesized with a high radiochemical yield (97%). The radiochemical purity of [^{99m}Tc]tricarbonyl Rabeprazole, according to the HPLC data, was 98%. As shown in Fig. 1b, the R_t values

Table 1. Effect of Rabeprazole amount on the radiochemical yield of [^{99m}Tc]tricarbonyl Rabeprazole[a]

Rabeprazole, μg	[^{99m}Tc]tricarbonyl Rabeprazole, %	Free ^{99m}Tc, %	$[^{99m}Tc(CO)_3(H_2O)_3]^+$ precursor
50	82.0 ± 0.11	5.0 ± 0.13	13.0 ± 0.19
100	84.0 ± 0.12	4.0 ± 0.16	12.0 ± 0.55
150	91.0 ± 0.18	3.3 ± 0.14	5.7 ± 0.19
200	98.0 ± 0.91	1.2 ± 0.58	0.8 ± 0.02
250	98.1 ± 0.12	1.4 ± 0.33	0.50 ± 0.06
300	97.5 ± 0.66	1.3± 0.20	1.2 ± 0.04
400	97.4 ± 0.11	1.2 ± 0.14	1.4 ± 0.29

[a] Values represent the mean ± SEM, $n = 3$.

Table 2. Biodistribution of [^{99m}Tc]tricarbonyl Rabeprazole in normal mice (% ID/g at indicated time post injection)[a]

Organs and body fluids	5 min	30 min	1 h	2 h
Blood	18.19 ± 0.44	8.31 ± 0.11	3.77 ± 0.15	2.15 ± 0.12
Bones	1.12 ± 0 .18	1.10 ± 0.12	0.98 ± 0.001	0.91 ± 0.001
Muscles	1.30 ± 0.01	1.20 ± 0.02	1.00 ± 0.01	0.94 ± 0.02
Liver	3.66 ± 0.12	17.55 ± 0.02	28.6 ± 0.15	12.16 ± 0.29
Lungs	1.22 ± 0.14	1.10 ± 0.02	1.0 ± 0.02	0.99 ± 0.01
Heart	1.55 ± 0.02	1.45 ± 0.01	1.11 ± 0.01	0.95 ± 0.01
Stomach	4.11 ± 0.11	7.9 ± 0.02	9.50 ± 0.22	5.54 ± 0.01
Intestine	2.70 ± 0.02	3.44 ± 0.15	4.18 ± 0.12	1.66 ± 0.05
Kidneys	2.99 ± 0.24	4.11 ± 0.15	6.33 ± 0.17	3.11 ± 0.29
Spleen	1.23 ± 0.16	1.11 ± 0.03	0.97 ± 0.04	0.91 ± 0.05
Thyroid	1.22 ± 0.15	1.10 ± 0.01	0.98 ± 0.01	0.90 ± 0.01

[a] Values represent mean ± SEM, $n = 5$; the same in Tables 3–5.

Table 3. Biodistribution of [^{99m}Tc]tricarbonyl Rabeprazole in ulcer-bearing mice (microbial model) (% ID/g at indicated time post injection)

Organs and body fluids	5 min	30 min	1 h	2 h
Blood	19.14 ± 0.25	9.11 ± 0.14	3.12 ± 0.14	2.12 ± 0.18
Bones	1.17 ± 0.13	1.13 ± 0.16	0.96 ± 0.003	0.93 ± 0.002
Muscles	1.40 ± 0.06	1.30 ± 0.03	1.11 ± 0.03	0.98 ± 0.01
Liver	4.11 ± 0.18	17.15 ± 0.33	26.15 ± 0.19	11.33 ± 0.20
Lungs	1.25 ± 0.12	1.14 ± 0.07	1.10 ± 0.03	0.97 ± 0.00
Heart	1.50 ± 0.01	1.22 ± 0.06	1.00 ± 0.04	0.99 ± 0.00
Stomach	10.15 ± 0.69	18.56 ± 0.87	35.30 ± 0.43	30.12 ± 0.08
Intestine	3.11 ± 0.06	4.11 ± 0.13	5.10 ± 0.19	1.23 ± 0.07
Kidneys	3.11 ± 0.28	4.18 ± 0.13	6.77 ± 0.13	3.18 ± 0.20
Spleen	1.20 ± 0.02	1.13 ± 0.01	0.99 ± 0.07	0.90 ± 0.02
Thyroid	1.17 ± 0.02	1.11 ± 0.03	1.00 ± 0.02	0.98 ± 0.00

Table 4. Biodistribution of [^{99m}Tc]tricarbonyl rabeprazole in ulcer- bearing mice (chemical model) (% ID/g at indicated time post injection)

Organs and body fluids	5 min	30 min	1 h	2 h
Blood	20.19 ± 0.66	9.16 ± 0.19	3.17 ± 0.19	2.15 ± 0.11
Bones	1.15 ± 0.17	1.12 ± 0.19	0.90 ± 0.00	0.88 ± 0.00
Muscle	1.30 ± 0.08	1.10 ± 0.01	1.0 ± 0.01	0.90 ± 0.00
Liver	4.15 ± 0.19	18.11 ± 0.65	25.17 ± 0.18	10.29 ± 0.90
Lungs	1.20 ± 0.11	1.11 ± 0.09	1.00 ± 0.01	0.90 ± 0.00
Heart	1.40 ± 0.07	1.20 ± 0.04	1.11 ± 0.06	0.90 ± 0.00
Stomach	8.10 ± 0.22	12.77 ± 0.24	23.70 ± 0.28	20.15 ± 0.60
Intestine	3.27 ± 0.12	4.55 ± 0.27	5.12 ± 0.15	1.29 ± 0.09
Kidneys	3.15 ± 0.20	4.13 ± 0.18	6.12 ± 0.12	3.12 ± 0.02
Spleen	1.25 ± 0.06	1.12 ± 0.04	0.95 ± 0.00	0.91 ± 0.00
Thyroid	1.11 ± 0.01	1.00 ± 0.02	0.98 ± 0.00	0.96 ± 0.00

for of free [^{99m}Tc]tricarbonyl and [^{99m}Tc]tricarbonyl rabeprazole were 4.5 and 9 min, respectively.

Reaction optimization. The reaction conditions, namely, pH of the reaction mixture, amount of the substrate used, and time, were optimized to achieve the radiochemical yield of 98.0%. Table 1 shows that, with an increase in the substrate amount, keeping the other conditions constant, the conversion to [^{99m}Tc]tricarbonyl rabeprazole increased up to 200 μg of rabeprazole (7.5 MBq) to reach the optimum radiochemical conversion of 98.0%. The pH of the labeling process is also a critical factor. pH 8 was found to be the most effective, ensuring the stability of [^{99m}Tc]tricarbonyl rabeprazole. The effect of the reaction time was also investigated; the radiochemical conversion of 98.0% was reached in 30 min. Finally, in vitro studies of the stability of [^{99m}Tc]tricarbonyl rabeprazole in rat serum were performed. The complex was found to be stable in serum for up to 12 h, after which the purity dropped to 90.0% at 24 h [97–109].

Biodistribution study. The biodistribution of [^{99m}Tc] tricarbonyl rabeprazole in various organs and fluids of control animals is shown in Table 2. The average percent of injected dose per gram tissue (% ID/g ± SD) is used to express the radioactivity levels. Low thyroid uptake at all periods shows that [^{99m}Tc]tricarbonyl Rabeprazole, is stable in vivo. [^{99m}Tc]Tricarbonyl Rabeprazole is rapidly absorbed in most organs, including the stomach, bones, heart, lungs, blood, kidneys, intestine, and liver at 5 min post injection. The liver uptake increased to 28.6% at 60 min post injection and then declined to 12.16% at 2 h post-injection, demonstrating hepatobiliary excretion of [^{99m}Tc]tricarbonyl rabeprazole. [^{99m}Tc]Tricarbonyl rabeprazole had a maximum concentration of 9.5% in the stomach at 1 h post injection. The biodistribution of [^{99m}Tc]tricarbonyl rabeprazole in a microbial model of ulcerated mice is shown in Table 3. It is necessary to compare the [^{99m}Tc]tricarbonyl rabeprazole uptake in normal stomach and microbiologically and chemically induced ulcerated stomachs. The [^{99m}Tc]tricarbonyl

Table 5. Uptake of various agents in normal stomach and ulcerated stomach (% ID/g) and ulcerated/normal stomach ratios at 60 min post injection

Parameter	[^{99m}Tc]Tricarbonyl rabeprazole	[^{99m}Tc]Rabeprazole	[^{99m}Tc]panto-prazole	[^{99m}Tc]omepra-zole	[^{125}I]Omeprazole
Normal stomach uptake	9.50 ± 0.22	5.1 ± 0.02	5.2 ± 0.70	8.5 ± 0.60	22.1 ± 0.6
Ulcerated stomach uptake	35.30 ± 0.43	16.9 ± 0.6	14.2 ± 0.70	22.0 ± 0.60	35.0 ± 0.60
Ulcerated/normal stomach ratio	3.72 ± 0.16	3.31 ± 0.19	2.73 ± 0.13	2.59 ± 0.17	1.58 ± 0.16

Rabeprazole uptake in the ulcerated stomach (microbial model) was found to be much higher over time, reaching 35.3% ID/g at 60 min post injection. The biodistribution of [^{99m}Tc]tricarbonyl Rabeprazole in a chemically induced stomach ulcer animal model is shown in Table 4. The [^{99m}Tc]tricarbonyl Rabeprazole uptake increased significantly over time in a stomach ulcer (chemical model), reaching 23.7% ID/g at 60 min post injection. It is worth mentioning that the differences in the [^{99m}Tc]tricarbonyl Rabeprazole uptake in the stomach of the three models are due to variances in the number of H_2-histamine receptors present in each model individually. Our results indicate that the radiotracer, [^{99m}Tc]tricarbonyl Rabeprazole, has a higher % ID/g ± SD value than many previously reported radiotracers (common among proton pump inhibitors), such as [^{99m}Tc]Pantoprazole [7], [^{99m}Tc]Omeprazole [11], and [^{99m}Tc]Rabeprazole [12], showing the maximum ulcerated stomach uptake of 27.2% ID/g at 30 min, 22.0% ID/g at 60 min, and 33.4% ID/g at 30 min, respectively. In addition, Table 5 shows that [^{99m}Tc]tricarbonyl Rabeprazole has ulcerated (microbial model)/normal stomach ratio of 3.72 ± 0.16, exceeding that reached with [^{99m}Tc]Pantoprazole, [^{99m}Tc]Omeprazole, [^{99m}Tc] Rabeprazole, and [^{125}I]Omeprazole.

CONCLUSION

An optimized methodology for the synthesis of [^{99m}Tc]tricarbonyl Rabeprazole using a [^{99m}Tc]tricarbonyl precursor was developed, ensuring high yield and optimum radiochemical conversion of 98.0%. According to biodistribution assessments, [^{99m}Tc]tricarbonyl Rabeprazole at 60 min post injection showed a higher stomach ulcer uptake of 35.3% ID/g in the microbial model than in the normal and chemical models. This percentage of stomach ulcer uptake is higher than that of previously suggested agents such as [^{99m}Tc]Pantoprazole, [^{99m}Tc]Omeprazole, and [^{99m}Tc]Rabeprazole. Thus, [^{99m}Tc]tricarbonyl Rabeprazole shows promise as a selective radiotracer for stomach ulcer imaging.

REFERENCES

1. Törüner, M., Bektaş, M., Cetinkay, H., Soykan, I., and Ozden, A., *Turk. J. Gastroenterol.,* 2004, vol. 15, no. 4, pp. 225–228.
2. Zheng, M., Luan, S., Gao, S., Cheng, L., Hao, B., Li, J., Chen, Y., Hou, X., Chen, L., and Lim, H., *Oncotarget,* 2017, vol. 8, no. 24, pp. 39143–39153.
3. Kwon, D., Chae, J.B., Park, C.W., Kim, Y.S., Lee, S.M., Kim, S., E.J., Huh, I.H., Kim, D.Y., and Cho, K.D., *Arzneimittelforschung,* 2001, vol. 51, no. 3, pp. 204–213.
4. Sanad, M.H., Saleh, G.M., and Marzook, F.A., *J. Label. Compd. Radiopharm.,* 2017, vol. 60, pp. 600–607.
5. Sanad, M.H., Salama, D.H., and Marzook, F.A., *Radiochim. Acta,* 2017, vol. 105, pp. 389–398.
6. Sanad, M.H. and Challan, S.B., *Radiochemistry,* 2017, vol. 59, pp. 307–312. https://doi.org/10. 1134/S1066362217030158
7. Sanad, M.H. and Ibrahim, I.T., *Radiochemistry,* 2013, vol. 55, pp. 341–345.
8. Abolfazl, H., Mohammad, A.K., Masoumeh, H., and Mahmoud, T.A., *Monatsh. Chem.,* 2012, vol. 143, pp. 619–623.
9. Mohammad, A.K. and Abolfazl, H., *Iran J. Org. Chem.,* 2009, vol. 4, pp. 268–270.
10. Unak, P., Lambrecht, F.Y., Biber, F.Z., Medine, I.E., and Teksoz, S., *J. Radioanal. Nucl. Chem.,* 2004, vol. 261, no. 3, pp. 587–591.
11. Sanad, M.H., *Radiochemistry,* 2013, vol. 55, pp. 605–609.
12. Sanad, M.H. and Ibrahim, I.T., *Radiochemistry,* 2015, vol. 57, pp. 425–430.
13. Sanad, M.H. and Talaat, H.M., *Radiochemistry,* 2017, vol. 59, pp. 396–401.
14. Sanad, M.H., Rizvi, F.A., and Kumar, R.R., *Radiochemistry,* 2020, vol. 62, no. 1, pp. 119–124.
15. Sanad, M.H., Safaa, B.C., Fawzy, A.M., Sayed, M., A.A., and Ebtisam, A.M., *Radiochim. Acta,* 2021, vol. 109, no. 2, pp. 109–117.
16. Alberto, R., Schibli, R., and Schubiger, A.P., *J. Am. Chem. Soc.,* 1999, vol. 121, no. 25, pp. 6076–6077.
17. Lipowska, M., Klenc, J, Marzilli, L.G., and Taylor, A.T., *J. Nucl. Med.,* 2012, vol. 53, no. 8, pp. 1277–1283.
18. Yoshiharu, K., Koji, I., and Jiro, T., *Ann. Nucl. Med.,* 1999, vol. 13, no. 2, pp. 127–132.
19. Taylor, A.T., Lipowska, M., and Marzilli, L.G., *J. Nucl. Med.,* 2010, vol. 51, no. 3, pp. 391–396.
20. Klenc, J., Lipowska, M., Taylor, A.T., and Marzilli, L.G., *Eur. J. Inorg. Chem.,* 2012, vol. 2012, no. 27, p. 4334.
21. Sanad, M.H. and Borai, E.H., *Radiochim. Acta,* 2015, vol. 103, no. 12, pp. 879–891.
22. Duangporn, W., *World J. Gastroenterol.,* 2014, vol. 20, no. 21, pp. 6420–6424.
23. Shah, S.Q., Khan, M.R., Ali, S.M., *Nucl. Med. Mol. Imag,* 2011, vol. 45, pp. 248–254.
24. Unak, P., Lambrecht, F.Y., Biber, F.Z., Medine, I.E., and

Teksoz, S., *J. Radioanal. Nucl. Chem.,* 2004, vol. 261, no. 3, pp. 587–591.

25. Klenc, J., Lipowska, M., Taylor, A.T., and Marzilli, L.G., *Eur. J. Inorg. Chem.,* 2012, vol. 2012, no. 27, p. 4334.
26. Sanad, M.H., El-Bayoumy, A.S.A., and Ibrahim, A.A., *J. Radioanal. Nucl. Chem.,* 2017, vol. 311, no. 1, pp. 1–14.
27. Taylor, A.T., Lipowska, M., and Marzilli, L.G., *J. Nucl. Med.,* 2010, vol. 51, no. 3, pp. 391–396.
28. Alberto, R., Schibli, R., and Schubiger, A.P., *J. Am. Chem. Soc.,* 1999, vol. 121, no. 25, pp. 6076–6077.
29. Lipowska, M., Klenc, J., Marzilli, L.G., and Taylor, A.T., *J. Nucl. Med.,* 2012, vol. 53, no. 8, pp. 1277–1283.
30. Duangporn, W., *World J. Gastroenterol.,* 2014, vol. 20, no. 21, pp. 6420–6424.
31. Rhodes, B.A., *Semin. Nucl. Med.,* 1974, vol. 4, p. 281.
32. Motaleb, M.A., Wanis, K.F., and Sanad, M.H., *Arab Journal of Nuclear Sciences and Applications,* 2005, vol. 38, pp. 137–145.
33. Motaleb, M.A., Wanis, K.F., and Sanad, M.H., *Arab Journal of Nuclear Sciences and Applications,* 2006, vol. 39, pp. 84–91.
34. EI-Wetery, A.S.A., Fayz, M.A.A., Sanad, M.H., and EIHashash, M.A.M., *Arab Journal of Nuclear Sciences and Applications,* 2007, vol. 40, pp. 109–118.
35. Motaleb, M.A. and Sanad, M.H., *Arab Journal of Nuclear Sciences and Applications,* 2012, vol. 45, pp. 71–77.
36. Ibrahim, I.V. and Sanad, M.H., *Radiochemistry,* 2013, vol. 55, pp. 336–340.
37. Abdel-Ghaney, I.Y. and Sanad, M.H., *Radiochemistry,* 2013, vol. 55, pp. 418–422.
38. Sanad, M.H. and Amin, A.M., *Radiochemistry,* 2013, vol. 55, pp. 521–526.
39. Sanad, M.H., *Radiochemistry,* 2013, vol. 55, p. 44.
40. Sanad, M.H. and El-Tawoosy, M., *J. Radioanal. Nucl. Chem.,* 2013, vol. 298, pp. 1105–1109.
41. Amin, A.M., Sanad, M.H., and Abd-Elhaliem, S.M., *Radiochemistry,* 2013, vol. 55, pp. 624–628.
42. Sanad, M.H., Borai, E.H., Fouzy, A.S.M. *IOSR Journal of Environmental Science, Toxicology and Food Technology,* 2014, vol. 8 (12), pp. 10–17.
43. Sanad, M.H., *J. Anal. Sci. Technol.,* 2014, vol. 5, p. 23.
44. Sanad, M.H. and Emad, H.B., *J. Anal. Sci. Technol.,* 2014, vol. 5, p. 32.
45. Sanad, M.H. and Shweeta, H.A., *J. Mol. Imag. Dynamic,* 2015, vol. 5, pp. 1–6.
46. Sanad, M.H., Abelrahman, M.A., and Marzook, F.M.A., *Radiochim. Acta,* 2016, vol. 104, pp. 345–353.
47. Borai, E.H., Sanad, M.H., and Fouzy, A.S.M., *Radiochemistry,* 2016, vol. 58, pp. 84–91.
48. Moustapha, M.E., Motaleb, M.A., and Sanad, M.H., *J. Radioanal. Nucl. Chem.,* 2016, vol. 309, pp. 511–516.
49. El-Kawy, O.A., Sanad, M.H., and Marzook, F., *J. Radioanal. Nucl. Chem.,* 2016, vol. 308, no. 1, p. 279.
50. Motaleb, M.A., Adli, A.S.A., El-Tawoosy, M., Sanad, M.H., and AbdAllah, M., *J. Label Compd. Radiopharm.,* 2016, vol. 59, pp. 157–163.
51. Sanad, M.H., Sallam, Kh.M., Marzook, F.A., and Abd-Elhaliem, S.M., *J. Label Compd. Radiopharm.,* 2016, vol. 59, pp. 484–491.
52. Franken, K., Mitrovic, M., van Diemen, C., *P. Gastroenterol,* 2012, vol. 7, pp. 1–8.
53. Sanad, M.H., Saad, M.M., Fouzy, A.S.M., Marzook, F., and Ibrahim, I.T., *J. Mol. Imag. Dynamic,* 2016, vol. 6, p. 1
54. Sanad, M.H., Ayman, F., and Dina, H., *Egypt. J. Rad. Sci. Applic.,* 2017, vol. 30, pp. 131–143.
55. Sanad, M.H., Hanan, T., and Gehan, S., *Egypt. J. Rad. Sci. Applic.,* 2017, vol. 30, pp. 117–130.
56. Sanad, M.H., Marzook, E.A.O.A., and El-Kawy, O.A., *Radiochemistry,* 2017, vol. 59, pp. 624–629.
57. Sanad, M.H., Sakr, T.M., Walaa, H.A.A., and Marzook, E.A., *J. Radioanal. Nucl. Chem.,* 2017, vol. 314, pp. 1505–1515.
58. Sanad, M.H., El-Tawoosy, M., and Ibrahim, I.T., *Radiochemistry,* 2017, vol. 59, pp. 92–97.
59. Sanad, M.H., Farouk, N., and Fouzy, A.S.M., *Radiochim. Acta,* 2017, vol. 105, pp. 729–737.
60. Ibrahim, I.T., Abdelhalim, S.M., Sanad, M.H., and Motaleb, M.A., *Radiochemistry,* 2017, vol. 59, pp. 301–306.
61. Motaleb, M.A., Selim, A.A., El-Tawoosy, M., Sanad, M.H., and El-Hashash, M.A., *J. Radioanal. Nucl. Chem.,* 2017, vol. 314, pp. 1517–1522.
62. Sanad, M.H., Sallam, K.M., and Marzook, F., *Radiochemistry,* 2017, vol. 59, pp. 525–529.
63. Sanad, M.H., Marzook, E.A., and Challan, S.B., *Radiochim. Acta,* 2018, vol. 106, pp. 329–336.
64. Sanad, M.H. and Alhussein, A.I., *Radiochim. Acta,* 2018, vol. 106, pp. 229–238.
65. Tamer, M.S., Sanad, M.H., Walaa, H.A., Dina, H.S., and Gehan, M.S., *Applied Radiation and Isotopes,* 2018, vol. 137, pp. 41–49.
66. Sanad, M.H., Farag, A.B., and Dina, H.S.J., *J. Label Compd. Radiopharm.,* 2018, vol. 61, pp. 501–508.
67. Sanad, M.H., Sallam, K.M., and Salama, D.H., *Radiochemistry,* 2018, vol. 60, pp. 58–63.
68. Sanad, M.H., Hanan, T., Ibrahim, I.T., Gehan, S., and Abozaid, L.A., *Radiochim. Acta,* 2018, vol. 106, p. 751.

69. Motaleb, M.A., Sanad, M.H., Selim, A.A., El-Tawoosy, M., and El-Hashash, M.A., *Radiochemistry,* 2018, vol. 60, pp. 201–207.
70. Motaleb, M.A., Sanad, M.H., Selim, A.A., El-Tawoosy, M., and El-Hashash, M.A., *International Journal of Radiation Biology, 2018*, vol. 94, pp. 590–596.
71. Sanad, M.H., Ibrahim, A.A., and Talaat, H.M., *J. Radioanal. Nucl. Chem.,* 2018, vol. 315, pp. 57–63.
72. Sanad, H.M. and Ibrahim, A.A., *Radiochim. Acta,* 2018, vol. 106, pp. 843–850.
73. Sanad, M.H., Farag, A.B., and Motaleb, M.A., *Radiochim. Acta,* 2018, vol. 106, pp. 1001–1008.
74. Sanad, M.H., Fouzy, A., S.M., Sobhy, H.M., Hathout, A.S., and Hussain, O.A., *Int. J. Radiat. Biol.,* 2018, vol. 94, pp. 1151–1158.
75. Sanad, M.H., Farag, A.B., and Saleh, G.M., *Radiochemistry,* 2019, vol. 61, pp. 347–351.
76. Sanad, M.H., Rizvi, F.A., Kumar, R.R., and Ibrahim, A.A., *Radiochemistry,* 2019, vol. 61, pp. 754-758.
77. Sanad, M.H., Marzook, F.A., Gehan, S., Farag, A.B., and Talaat, H.M., *Radiochemistry,* 2019, vol. 61, pp. 478-482.
78. Rizvi, S.F.A., Zhang, H., Mehmood, S., and Sanad, M.H., *Translational Oncology,* 2020, vol. 13, p. 100854.
79. Sanad, M.H., Abdel Rahim, E.A., Rashed, M.M., et al., *World Journal of Pharmacy and Pharmaceutical Sciences,* 2020, vol. 9(8), pp. 148–158.
80. Sanad, M.H., Marzook, F.A., and Abd-Elhaliem, S.M., *Radiochim. Acta,* 2021, vol. 109, pp. 41–46.
81. Sanad, M.H., Rizvi, S.F.A., and Farag, A.B., *Radiochim. Acta,* 2021, vol. 109(6), pp. 477–483.
82. Sanad, M.H., Farag, A.B., and Rizvi, S.F.A., *Radiochimica Acta,* 2021, vol. 109 (7), pp. 575–582.
83. Sanad, M.H., Gizawy, M.A., Motaleb, M.A., Ibrahim, I.T., and Saad, E.A., *Radiochemistry,* 2021, vol. 63(4), pp. 507–514.
84. Sanad, M.H., Marzook, F.A., Rizvi, S.F.A., Farag, A.B., and Fouzy, A.S.M., *Radiochemistry,* 2021, vol. 63, pp. 520–525.
85. Sanad, M.H., Eyssa, H.M., Gomaa, N.M., Marzook, F.A., and Bassem, S.A., *Radiochimica Acta,* 2021, vol. 109, pp. 711–718.
86. Sanad, M.H., Rizvi, S.F.A., and Farag, A.B., *Chem Biol Drug Des.,* 2021, vol. 98, pp. 751–761.
87. Sanad, M.H., Eyssa, H.M., Marzook, F.A., et al., *Radiochemistry,* 2021, vol. 63 (5), pp. 635–641.
88. Sanad, M.H., Eyssa, H.M., Marzook, F.A., et al., *Radiochemistry,* 2021, vol. 63, pp. 642–650.
89. Sanad, M.H., Eyssa, H.M., Marzook, F.A., et al., Radiochemistry 2021, vol. 63, no. 6, pp. 835–842.
90. Sanad, M.H., Eyssa, H.M., Marzook, F.A., et al., *Radiochemistry,* 2021, vol. 63, no. 6, pp. 811–819.
91. Campieri, M., *Gut*, 2001, vol 48, pp. 132–135.
92. Sanad, M.H., Emam, A., Amal, S.H., Omaima, H., Magdy, R., and Ahmed, F., *Egyptian J. Chem.,* 2022, vol. 65(3), pp. 203–214.
93. Sanad, M.H., Rizvi, S.F.A., and Farag, A.B., *Chemical Papers,* 2022, vol. 76, no. 2, pp. 1253–1263.
94. Sanad, M.H., Farag, A.B., Marzook, F.A., and Mandal, S.K., *Radiochim. Acta,* 2022, vol. 110. pp. 67–74.
95. Sanad, M.H., Nermien, M.G., Nermeen, M.E., Ismail, T.I., and Ayman, M., *J. Label Compd. Radiopharm.,* 2022, vol. 65(3), pp. 71–82.
96. Eyssa, H.M., Heba, M.E., and Sanad, M.H., *Radiochim. Acta,* 2022, vol. 110(3), pp. 205-218
97. Sanad, M.H., Fawzy, A.M., Ayman, B.F., Sudip, K.M., Syed, F.A.R., and Jeetendra, K.G., *Radiochim. Acta,* 2022, vol. 110 (4), pp. 267-277
98. Sanad, M.H., *Ulcerative Colitis and Peptic Ulcer Imaging,* Germany: LAP LAMBERT Academic Publishing, 2017.
99. Sanad, M.H., *Nuclear Medicine and Brain Imaging,* Germany: LAP LAMBERT Academic Publishing, 2017.
100. Ayman, F., Ping, W., Mahmoud, A., and Hesham, S., *Biological and Medical Chemistry,* 2021, vol. 12003930, https://doi. org/10. 26434/chemrxiv
101. Galal, H.E., Nahed, M.F., Ayman, B., and Sheikha, A.A., *Nucleoside & Nucleotide and Nucleic Acid,* 2018, vol. 7, pp. 186–198.
102. Elgemeie, G.H., Fathy, N.M., Farag A.B., and Yahab, I.B., *Nucleoside & Nucleotide and Nucleic Acid,* 2020, vol. 39, pp. 1–16.
103. Farag, A.B., Ewida, H.E., Ahmed, M.S., *European Journal of Medicinal Chemistry,* 2018, vol. 148, pp. 73–85.
104. Elgemeie, G.H., Fathy, N.M., Farag, A.B., and Kursani, S.A., *Nucleoside & Nucleotide and Nucleic Acid,* 2018, vol. 37, pp. 186–198.
105. Elgemeie, G.H. and Farag, A.B., *Nucleoside & Nucleotide and Nucleic Acid,* 2017, vol. 36, pp. 328-342.
106. Elgemeie, G.H., Fathy, N.M., Farag, A.B., Kursani, S.A., *Nucleoside & Nucleotide and Nucleic Acid,* 2017, vol. 36, pp. 355–377.
107. Elgemeie, G.H., Fathy, N.M., Zaghary, W.A., and Farag, A.B., *Nucleoside & Nucleotide and Nucleic Acid,* 2017, vol. 36, pp. 198–212.
108. Rizvi, S.F.A., Jabbar, T., Shahid, W., Sanad, M.H., and Zhang, H., *Applied Biochemistry and Biotechnology,* 2022, 1-12. https://doi.org/10. 1007/s12010-022-03856-1
109. Sanad, M.H., Farag, A.B., Bassem, S.A., and Marzook, F.A., *Toxicology Reports,* 2022, vol. 9, pp. 470–479